PHILOSOPHICAL TRANSACTIONS OF THE ROYAL SOCIETY A MATHEMATICAL, PHYSICAL & ENGINEERING SCIENCES

Formation of Microstructure in Polymer Blends [and Discussion]

J. S. Higgins, A. Keller, C. B. Bucknall and A. H. Windle

Phil. Trans. R. Soc. Lond. A 1994 **348**, 131-147
doi: 10.1098/rsta.1994.0085

Formation of microstructure in polymer blends†

By J. S. Higgins

Department of Chemical Engineering and Chemical Technology, Imperial College of Science, Technology and Medicine, Prince Consort Road, London SW7 2BY, U.K.

The microstructure and morphology of a mixture of polymeric materials depends on factors in both the thermal and rheological history of a sample as well as on its equilibrium thermodynamics. Concentrating largely on systems which are partly miscible we explore the effects of molecular, rheological and thermodynamic parameters on phase diagrams of binary polymer blends and show how these interact with sample preparation in determining the final sample morphology.

1. Introduction

Many polymeric materials in current use are mixtures of two or more different chemical species. Examples are polystyrene with polyphenyl oxide, marketed by GE as Noryl, polystyrene with polybutadiene (known as high impact polystyrene) and thermoplastic–epoxy resin mixtures used as matrices in fibre composites. The first of these exists in a single-phase (in the thermodynamic sense) homogeneous blend (see, for example, Maconnachie *et al.* 1984), the second is an immiscible two-phase mixture where the polystyrene has been polymerized from monomer containing the unsaturated rubber to produce a system with rubber particles dispersed in a glass matrix (Kroschwitz 1990) while the last is a partly miscible system which has been frozen into a partly demixed state by the curing epoxy (Bucknall & Partridge 1986; Yamanaka & Inoue 1989; Kinloch *et al.* 1993).

In each case the level of miscibility and the consequent morphology of the sample has been tailored to obtain desirable physical properties in the final material.

In order to explore how the molecular thermodynamic and rheological parameters which govern polymer–polymer miscibility can be manipulated and exploited to give desirable morphologies and hence materials properties we will first discuss the basis theory of miscibility in binary polymer blends and the kinetics of the phase separation process. We will consider a number of specific examples where mixing or demixing in polymer blends produces changes in sample morphology.

† This paper was produced from the author's disk by using the TEX typesetting system.

Phil. Trans. R. Soc. Lond. A (1994) **348**, 131–147
Printed in Great Britain

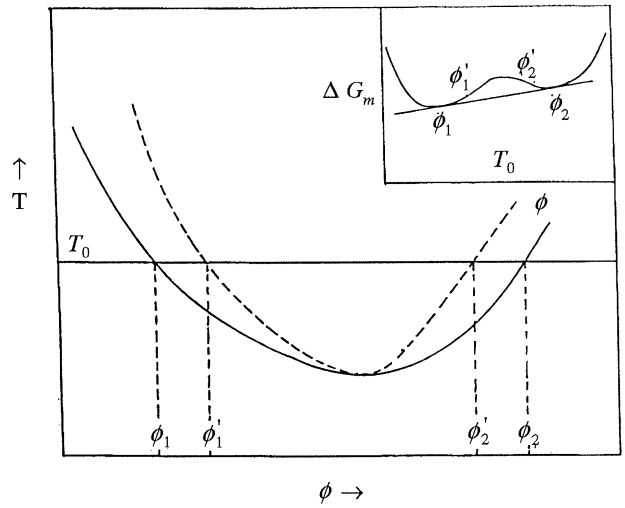

Figure 1. Theoretical phase diagram and (inset) ΔG_m for a binary polymer mixture exhibiting an LCST. Reprinted with permission from Higgins *et al.* (1989). Copyright American Chemical Society.

2. Thermodynamics of polymer blends

The free energy of mixing, ΔG_m for a polymer blend may be calculated from a wide number of models. One of the simplest and the one we will use here is the Flory–Huggins lattice model (Flory 1941). ΔG_m is here expressed per lattice segment and

$$\Delta G_m/RT = n_1 \ln \phi_1 + n_2 \ln \phi_2 + \phi_1 \phi_2 \chi_{12}, \tag{2.1}$$

where n_1 and n_2 are the molar numbers of polymers 1 and 2, respectively, ϕ_1 and ϕ_2 are the volume fractions of the components, χ_{12} is the interaction parameter. In the original Flory–Huggins theory χ_{12} was independent of concentration and inversely dependent on temperature. However, with such a simple description of χ_{12} equation (2.1) is unable to predict the behaviour of most real polymer systems. Either more complex equations of state models for ΔG_m must be invoked or equation (2.1) is used but with an empirical temperature and concentration-dependent χ_{12} (Eichinger & Flory 1968; Flory *et al.* 1964).

The inset in figure 1 is a typical dependence of ΔG_m on ϕ for a system that is partly miscible at the temperature of observation, T_o. The main diagram in figure 1 shows the corresponding miscibility limits in temperature and composition. Clearly, for any composition between ϕ_1 and ϕ_2 the system can reduce ΔG_m by separating into two phases with composition ϕ_1 and ϕ_2. The solid line in figure 1 is called the binodal and is defined by the points of common tangent to ΔG_m (i.e. ϕ_1 and ϕ_2 at T_o). At these compositions the chemical potentials μ_1 and μ_2 are equal and the two phases can coexist.

The dashed line is the spinodal, defined by the points of inflection where $\partial^2/\partial\phi^2(\Delta G_m) = 0$. These points are ϕ_1' and ϕ_2' in the inset. For compositions between ϕ_1' and ϕ_2', $\partial^2/\partial\phi^2(\Delta G_m) < 0$ and the system is unstable to all small concentration fluctuations. The phase-separation process is called spinodal decomposition. Between ϕ_1 and ϕ_1' and ϕ_2 and ϕ_2', $\partial^2/\partial\phi^2(\Delta G_m) > 0$ so that small fluctuations are damped out and phase separation proceeds by a nucleation and

growth process. For $\phi < \phi_1$ and $\phi > \phi_2$ the system is a stable single phase. The point where the binodal and spinodal meet is the critical point.

It is notable that this phase diagram is inverted compared with similar ones for low molecular mass systems. Lower critical solution temperatures are typical of high molecular mass polymer blends and arise because of the relative unimportance of the combinational entropy of mixing (the first two terms in equation (2.1) become very small as n_1 and n_2 become small). Also the diagram is not symmetrical. This again is typical and usually suggests $n_1 \neq n_2$ but may also indicate a complex variation of χ with ϕ.

It is the second derivative of ΔG_m with respect to ϕ that governs both the intensity of scattering in the single phase outside the binodal and the kinetics of phase separation inside the spinodal.

From equation (2.1) we obtain

$$\partial^2/\partial\phi^2(\Delta G_\mathrm{m}/RT) = (N_1\phi_1)^{-1} + (N_2\phi_2)^{-1} - 2\chi_{12}. \tag{2.2}$$

Here N_1 and N_2 are the number of lattice sites occupied by polymers 1 and 2 (given by the degree of polymerization if the lattice site is assumed to be occupied by a monomer of either polymer). If χ_{12} is concentration dependent, then we replace χ_{12} by χ_eff which we discuss in § 3*a*. Since the second derivative in equation (2.2) appears frequently throughout this paper, we have adopted a shorthand notation $G'' \equiv \partial^2/\partial\phi^2(\Delta G_\mathrm{m}/RT)$.

3. Scattering experiments to investigate blends and determine phase boundaries

A homogeneous one-phase polymer mixture is transparent and exhibits a single glass transition temperature (see Fernández *et al.* 1989).

A change in either of these two conditions is commonly used to determine the temperature composition range whether the sample becomes two phase. Clearly the existence of a cloud point curve depends both on the component polymers having different refractive indices and on the phase size being comparable with the wavelength of light, while the use of a dynamic mechanical parameter such as T_g depends on the two polymers having different T_gs to start with. Both criteria leave something to be desired if a precise phase boundary is to be compared with thermodynamic theory, although in practice they are regularly used. The determination of T_g is notoriously dependent on sample thermal history, and, while a cloud point temperature can be precisely determined, it, together with T_g determination, cannot indicate whether the sample has become two phase at the binodal (where the mixture is metastable) or at the spinodal. To answer these questions careful scattering experiments, either in the one- or in the two-phase region, are required.

(*a*) *Small-angle scattering from one-phase polymer blends*

It is well known (Einstein 1910; Debye & Bueche 1941) that the zero angle scattering from a homogeneous mixture is determined by the amplitude of the concentration fluctuations and hence is directly related to G''. In fact $S(0) = G''^{-1}$, so that, at the spinodal, the scattering becomes infinite (so-called critical scattering). This offers a means of directly determining G'' from scattering experiments. In fact light scattering is too sensitive to sample imperfections, X-ray scattering

PHILOSOPHICAL TRANSACTIONS OF THE ROYAL SOCIETY A MATHEMATICAL, PHYSICAL & ENGINEERING SCIENCES

poses difficulties in normalizing to absolute intensities, and for many hydrocarbons, gives insufficient intensity. It was the advent of small-angle neutron scattering which really opened up the possibility of observing G'' and, through a model such as equations (2.1) and (2.2) obtaining χ_{12} (Warner *et al.* 1983; Shibayama *et al.* 1985; Clark *et al.* 1993; Lapp *et al.* 1985; Higgins *et al.* 1989). Generally, to obtain a good intensity, one of the components must be deuterated, and then care must be taken in inferring from the results information about the analogous hydrogenous blends (Graessley *et al.* 1993; Atkin *et al.* 1982).

On the basis of mean-field theory (or the so-called random-phase approximation), it has been shown by a number of authors (Warner *et al.* 1983; Shibayama *et al.* 1985; Lapp *et al.* 1985) that normalized scattering per segment volume from a one-phase two-component system may be approximated to

$$S_{\mathrm{T}}^{-1}(Q) = S^{-1}(0)[1 + \tfrac{1}{3}Q^2R_{\mathrm{ap}}^2], \tag{3.1}$$

where

$$S^{-1}(0) = (N_1\phi_1)^{-1} + (N_2\phi_2)^{-1} - 2\chi_{12} = G''. \tag{3.2}$$

$Q = (4\pi/\lambda)\sin(\frac{1}{2}\theta)$, and R_{ap} is a function of both the radii of gyration of the component polymers and of χ_{12}. λ is the wavelength of the scattered neutrons.

$$R_{\mathrm{ap}}^2 = \left[\frac{R_{\mathrm{g1}}^2}{\phi_1 N_1} + \frac{R_{\mathrm{g2}}^2}{\phi_2 N_2}\right] S(0). \tag{3.3}$$

Analysis of SANS data in terms of equation (3.2) involves either extracting $S^{-1}(0)$ from the normalized forward scattered intensity, or choosing the best value of χ_{12} to fit the observed values of R_{ap} as a function of ϕ (Tomlins & Higgins 1988). The problem with this latter approach is its requirement for values of both the radii of gyration and degree of polymerization of the component polymers. Very careful normalization of the data is required to obtain reliable values of $S^{-1}(0)$, and particular attention must be paid to subtraction of incoherent scattering backgrounds.

Figure 2 shows the normalized scattering from a mixture of deuterated polymethylmethacrylate with solution chlorinated polyethylene (50/50 composition) at six temperatures. The lowest four are below the phase boundary while the higher two are inside it and the shape of their scattering will be discussed in the next section. The scattering from one of the polymers is also shown to demonstrate the level from a single-component system. As the phase boundary is approached, the intensity from the blends increases, as predicted by equation (3.2). Figure 3 shows the data plotted according to equation (3.1) so that G'' can be determined. Extrapolation of these values to $G''^{-1} = 0$ gives the spinodal temperature of this system at 113.6 °C (see figure 4) (Clark *et al.* 1993).

We do not have space here to discuss in detail the interpretation of G'' and its temperature dependence or the value of χ_{12} obtained by interpreting it in terms of equation (2.2). As already mentioned it is important to note, though, that if χ_{12} is composition dependent, then it should be replaced in equation (3.2) by χ_{eff}, where

$$\chi_{\mathrm{eff}} = \chi_{12} - (1 - 2\phi_1)\partial\chi_{12}/\partial\phi_1 - \tfrac{1}{2}\phi_1(1 - \phi_1)\partial^2\chi_{12}/\partial\phi_1^2 \tag{3.4}$$

(see, for example, Clark *et al.* 1993).

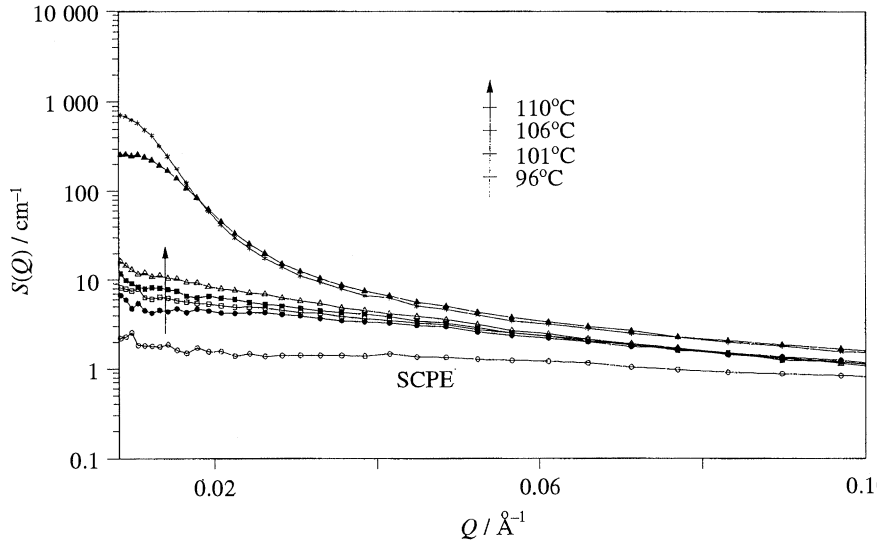

Figure 2. SANS patterns obtained for a solution chlorinated polyethylene sample and for a blend with polymethylmethacrylate at six different annealing temperatures. Four of the patterns correspond to the blend in the one-phase region: 96 °C; 101 °C; 106 °C; 110 °C. The two top curves correspond to the scattering from the same sample in the two-phase region: ?, 114 °C; 118 °C. For clarity, lines are shown connecting the experimental points. Reprinted with permission from Clarke *et al.* (1993). Copyright American Chemical Society.

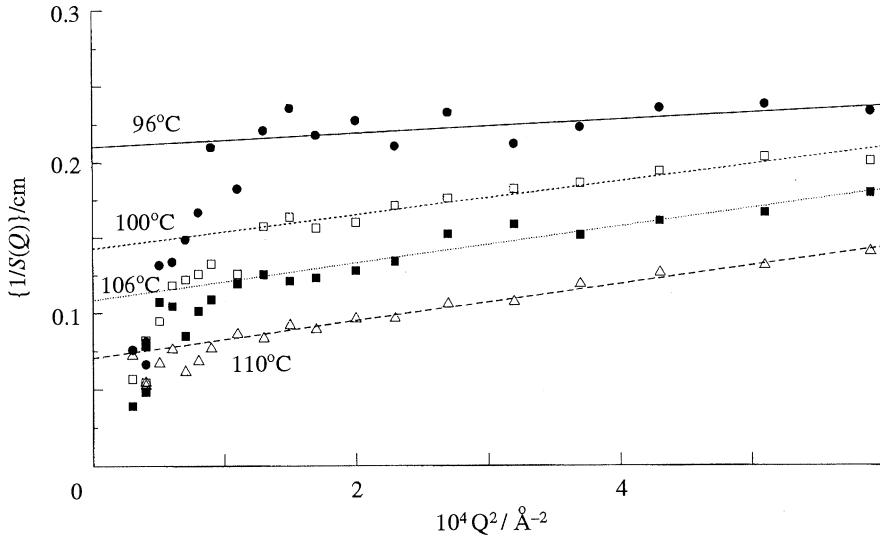

Figure 3. Plots of S against Q^2 for the blend as in figure 2 for four different temperatures in the one-phase region of the phase diagram. The lines correspond to the least-squares fit to the data. Reprinted with permission from Higgins *et al.* (1989). Copyright American Chemical Society.

(*b*) *Spinodal decomposition*

If an initially homogeneous sample is suddenly heated to temperatures inside the spinodal curve then phase separation proceeds via spinodal decomposition.

All concentration fluctuations become unstable and grow in amplitude with a wavelength (or wave vector) dependent growth rate. This growth rate, $R(Q)$,

PHILOSOPHICAL TRANSACTIONS OF THE ROYAL SOCIETY A MATHEMATICAL, PHYSICAL & ENGINEERING SCIENCES

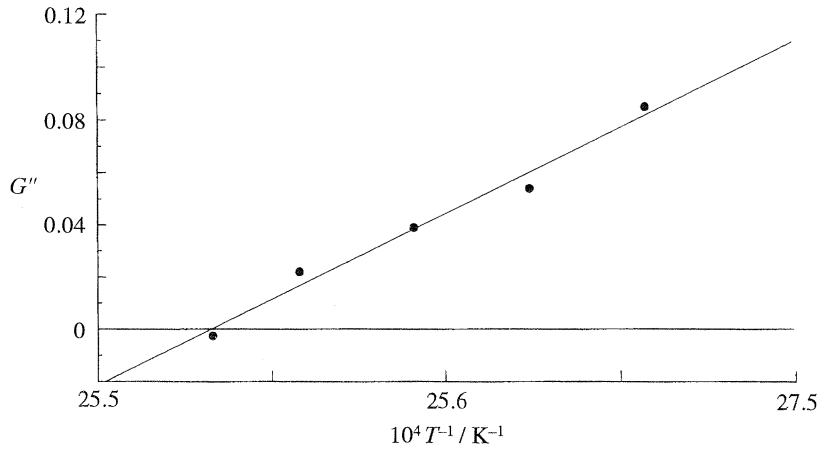

Figure 4. Plot of the second derivative of the Gibbs free energy of mixing as a function of inverse temperature for the blend as in figures 2 and 3. The line is a least-squares fit through the data.

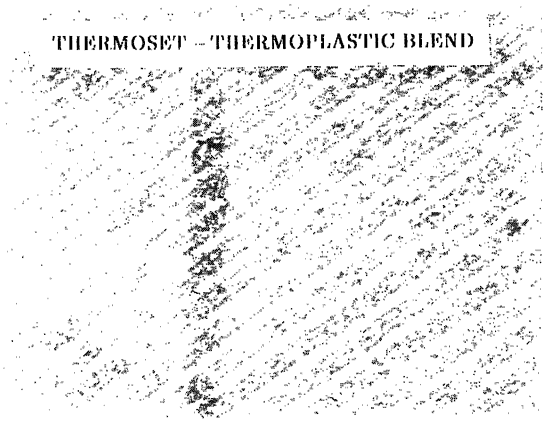

Figure 5. Optical micrograph of a Thermoset–thermoplastic blend provided by ICI plc. Magnification ×20.

has a maximum $R(Q_{\mathrm{m}})$, where $Q_{\mathrm{m}} = 2\pi/d_{\mathrm{m}}$ and d_{m} is the wavelength. As a consequence those wavelengths close to d_{m} grow fastest and the system separates into two coexisting phases with dimensions of order d_{m}. Material flows into the phases in what appears to be diffusion up the concentration gradient (because there is no activation energy for the process). The morphology of these phases is co-continuous, in the so-called spinodal structure. An example is shown in figure 5. All this refers to the very early stages – afterwards unless the structure is quenched in by cooling below T_{g}, or by chemical cross-linking as in figure 5, the phases begin to grow in size (d_{m} decreases and Q_{m} moves to smaller values) and eventually the spinodal structure begins to break up.

The spinodal decomposition process in polymer systems was modelled by Cahn and Hilliard (Cahn 1986; Huston *et al.* 1966). They derived a diffusion equation

$$-\partial\phi/\partial t = MG''\nabla^2\phi - 2MK\nabla^4\phi + \text{nonlinear terms}, \tag{3.5}$$

where M is the diffusional mobility of the system and the term K arises from the free energy in the concentration gradients. K is determined by the statistical segment lengths of the component polymers (see below).

The mobility term M has been the subject of considerable recent discussion (Jones 1987; Kramer & Composto 1984). While it evidently is governed by the mutual diffusion coefficients D_1 and D_2 of the component copolymers, the exact method of combination of D_1 and D_2 and the modification of each in the presence of the other polymer are not clear.

Equation (3.5) can be solved (if nonlinear terms are ignored) in terms of growth $R(Q)$ in amplitude of each Fourier component of the concentration fluctuations:

$$R(Q) = -MG''Q^2 - 2MKQ^4. \tag{3.6}$$

The function has a maximum at

$$Q_{\mathrm{m}} = \tfrac{1}{2}[G''/K]^{1/2}, \tag{3.7}$$

and for values of $Q > Q_{\mathrm{c}} = 2^{1/2}Q_{\mathrm{m}}$, $R(Q)$ becomes negative so that short wavelength fluctuations are damped out.

The scattered intensity from such a system grows exponentially with time as

$$S(Q,t) = S(Q,0)\exp[2R(Q)t], \tag{3.8}$$

where $R(Q)$ is given by equation (3.6). The coefficient of the first term on the right-hand side of equation (3.5) is identified as the Cahn–Hilliard diffusion coefficient, D:

$$D = M(-G'') = 2R(Q_{\mathrm{m}})/Q_{\mathrm{m}}^2. \tag{3.9}$$

The early stages of spinodal decomposition (where G'' does not differ too strongly from its initial value) are observed as an exponentially increasing scattered intensity, which develops a maximum at Q_{m}. During the early stages, Q_{m} is not time dependent and so the maximum remains at constant Q. D can be obtained from the intercept of a plot of $R(Q)/Q^2$ versus Q^2 following equation (3.6). These values extrapolate to zero at the spinodal temperature where $G'' = 0$. Extraction of the free energy term from equation (3.6) requires knowledge of M or K. Alternatively, values of G'' can be extrapolated from the one-phase region as described in § 3*a* and then used to check the theoretical predictions for K or to obtain the concentration dependence of M.

Equation (3.8) on which the analysis of $R(Q)$ is based, is actually a simplification because it omits the effect of thermal fluctuations in the system. While the effect of thermal fluctuations was originally developed by using the Cahn–Hilliard formalism, for convenience we follow (Binder 1983; Pincus 1981; Strobl 1985) and rewrite equation (3.5) in terms of the random-phase approximation including the thermal fluctuation term to obtain

$$\partial/\partial t(S(Q,t)) = 2MQ^2(S_{\mathrm{T}}^{-1}(Q)S(Q,t) - 1), \tag{3.10}$$

where $S_{\mathrm{T}}(T)$ is as defined in equation (3.1), but since G'' is negative inside the spinodal, $S_{\mathrm{T}}(Q)$ will be negative for part of the Q range and therefore not observable experimentally. The solution of equation (3.10) is

$$S(Q,t) = \{S(Q,0) - S_{\mathrm{T}}(Q)\}\exp(2R(Q)t) + S_{\mathrm{T}}(Q), \tag{3.11}$$

where

$$R(Q) = -MQ^2 S_{\mathrm{T}}^{-1}(Q), \tag{3.12}$$

and substituting from equation (3.1)–(3.3), we find

$$R(Q) = -MQ^2\{G'' + \tfrac{1}{3}Q^2[R_{\mathrm{g}1}^2/\phi_1 N_1 + R_{\mathrm{g}2}^2/\phi_2 N_2]\}. \tag{3.13}$$

Comparison with equation (3.7) now allows us to identify K.

$$K = \tfrac{1}{6}[R_{\mathrm{g}1}^2/\phi_1 N_1 + R_{\mathrm{g}2}^2/\phi_2 N_2]. \tag{3.14}$$

Thus K is obtained from the slope of the plots in figure 3.

Given that the ratio $R_{\mathrm{g}}^2/M_{\mathrm{w}}$ is quoted in the literature for a number of bulk polymers and ignoring complications such as polydispersity effects or changes in conformation in the blend, we write

$$K = \tfrac{1}{6}m_1\left[\frac{(R_{\mathrm{g}}^2/M_{\mathrm{w}})_1}{\phi_1} + \frac{(R_{\mathrm{g}}^2/M_{\mathrm{w}})_2}{\phi_2}\frac{m_2}{m_1}\right], \tag{3.15}$$

where m_1 and m_2 are monomer masses of the two polymers.

Now that we see that the two factors governing phase separation morphology, G'' and K (equation (3.7)), are determined by the equilibrium thermodynamics observed in the one-phase region. G'' may be obtained from the intercept and K the slope of data such as that in figure 3.

Equation (3.7) shows us that Q_{m} will be large for large values of G'' (i.e. well away from the spinodal) and for small values of K (i.e. very flexible polymer molecules). Since Q_{m} is inversely related to the real-space structural distance d_{m} ($d_{\mathrm{m}} = 2\pi/Q_{\mathrm{m}}$) deep quenches of flexible molecules should give small phase sizes while shallow quenches of stiffer molecules should correspond to larger phases.

The only unknown in equation (3.1) is $S(Q, 0)$. Now this is the scattered intensity at time zero, which presumably for an infinitely sharp temperature jump, is the scattered intensity at the temperature before the jump. This is just $S_{\mathrm{T}}(Q)$ again as in equation (3.1) but with a value of G'' appropriate to this prejump temperature. Since, now, two values of G'' will be necessary parameters, we identify that in the one-phase region (prejump) as G_{i}'' and that in the two-phase region (postjump) as G_{f}''. Of course, real temperature jumps are not infinitely sharp, and G_{i}'' may reflect a whole range of intermediate temperatures. Binder has explored by computer simulation the effect of 'slow' jumps (Carmesin *et al.* 1986).

It has been found (see, for example, Higgins *et al.* 1989) that the effect of $S_{\mathrm{T}}(Q)$ is generally quite small except for very shallow quenches. $S_{\mathrm{T}}(Q)$ is called the virtual structure factor since it cannot be measured directly, and is in fact negative over part of the Q-range. It can only be obtained by extrapolating data such as that in figure 3 at each Q-value against temperature to the desired temperature inside the spinodal. Because of this difficulty and the observation that $S_{\mathrm{T}}(Q)$ is usually small, data from samples undergoing spinodal decomposition are usually interpreted via equation (3.8) rather than equation (3.11) and this may lead to some of the discrepancies between the data and the Cahn–Hilliard theory.

Figure 6 shows the time variation of the intensity of light scattered by a polymer mixture which has been rapidly heated to within the spinodal. By about 85 s after the jump the maximum in the intensity is clearly visible. Initially it grows at fixed Q but by about 150 s it is beginning to move to lower Q in the late stages of

PHILOSOPHICAL TRANSACTIONS OF THE ROYAL SOCIETY A MATHEMATICAL, PHYSICAL & ENGINEERING SCIENCES

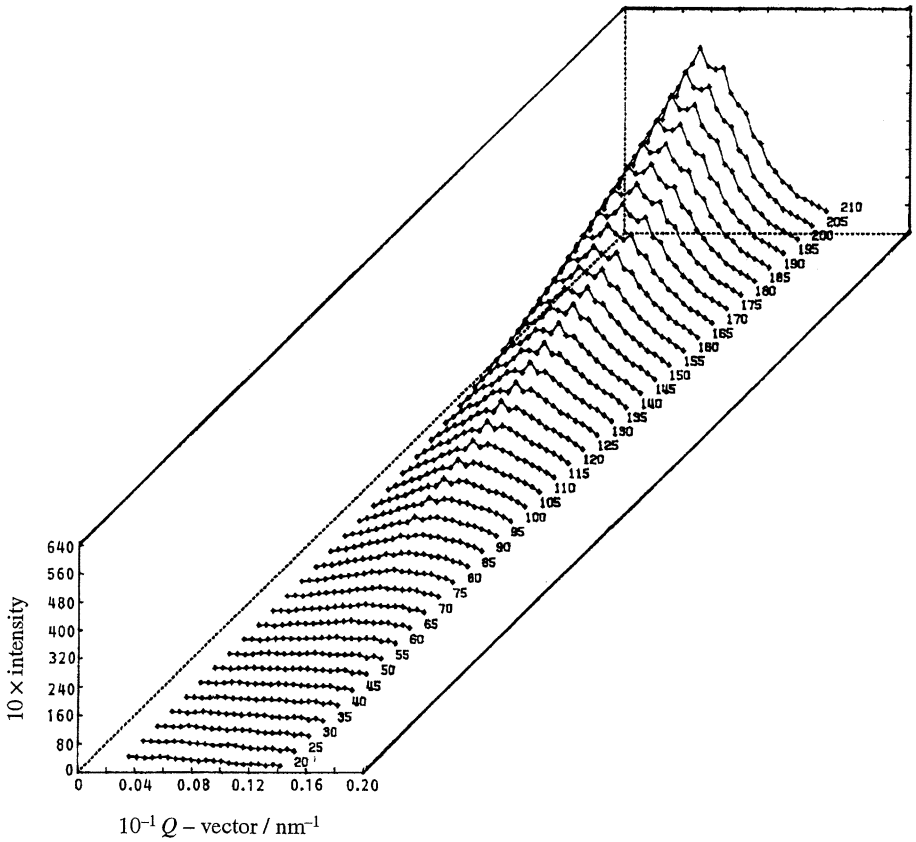

Figure 6. A typical series of intensity against time plots for a 50/50 blend of tetramethylbisphenol-A-polycarbonate with polystyrene which was rapidly heated to 242 °C (within the phase boundary at time zero. Reprinted from Guo & Higgins (1990) with permission from Butterworth Heinemann.

spinodal decomposition. If this sample is quenched below T_g of the two polymers and examined in a microscope, structure such as that in figure 5 is observed.

To obtain the growth rate $R(Q)$ from such intensity values, the intensity of each Q value is plotted semilogarithmically against time. Figure 7 shows $R(Q)$ against Q for the same sample as in figure 6 but at various temperatures inside the spinodal. As predicted by equation (3.7) Q_m moves to higher Q as the temperature increases, i.e. deeper inside the spinodal, as G'' increases from zero at the spinodal. Indeed data from such observations can be used to obtain information about the spinodal temperature. It has already been mentioned that $\bar{D}$ should extrapolate to zero at the spinodal, but so also should Q_m itself.

The gross features of spinodal decomposition as shown in figure 5, 6 and 7 are regularly observed when high molecular mass polymer mixtures are heated above the phase diagram. The details of the Cahn–Hilliard theory as presented by equations (3.6)–(3.9) are not followed in practice. For example, if the data in figure 7 are plotted accordingly to equation (3.6) as $R(Q)/Q^2$ against Q^2 straight lines are correctly obtained. However, the slope $(-2MK)$ and intercept (MG'') of these lines can be used to calculate Q_m, and the values of Q_m so

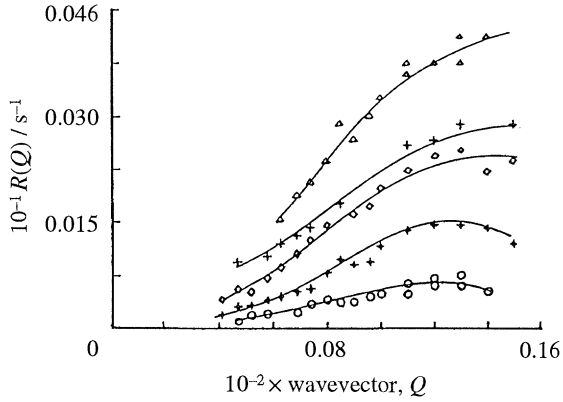

Figure 7. Plot of growth rate $R(Q)$ against Q for the TMPC/PS-5 (50/50) mixture as in figure 6 at different temperatures. 234 °C; 236 °C; 238 °C; 240 °C; 242 °C. Reprinted from Guo & Higgins (1990) with permission from Butterworth Heinemann.

obtained neither agree with those observed directly in figure 6 nor show the correct temperature dependence. Such discrepancies are regularly observed in practice and can be attributed to many factors: use of equation (3.8) rather than equation (3.11) to describe the data (Okada & Han 1986); the simplification of the Cahn-Hilliard theory to consider only linear terms (Snyder & Meakin 1985); the non-instantaneous nature of the temperature jump preceeding phase separation (Carmesin *et al.* 1986). It is also possible that for a particular system either G'' or K are showing unusual temperature dependence. Such a possibility has been suggested for the system shown in figures 6 and 7 (Guo & Higgins 1989; Brereton *et al.* 1993).

There is evidently a large and expanding literature exploring the experimental and theoretical details of the spinodal decomposition process. An excellent recent review has been given by Hashimoto (1993).

4. G'' and its control of morphology

While the details of the spinodal decomposition observed have yet to be thoroughly understood theoretically, it is already clear that the main parameters governing the morphology of a sample will be G'' and K (i.e. Q_{m} in equation (3.7)). For the majority of blends studied the polymers are flexible coils and the values of K are very similar so it is G'' which provides the controlling parameter for the phase separation. We have already seen that G'' can be obtained from small angle neutron scattering experiments in the one phase region. Equation (3.7) shows that if we believe we can determine K in the blend from the values of $R_{\mathrm{g}}^2/M_{\mathrm{w}}$ in the single component (as in equation (3.14) or (3.15)) then G'' can also be obtained from observation of the spinodal decomposition process. Figure 8 shows an example where data from the two types of experiment were obtained on the same system by neutron scattering.

Such a comparison of data is not usually possible since the one-phase region is explored by neutrons on a deuterated sample and the spinodal decomposition is normally explored by light scattering from ordinary samples. In this case the

PHILOSOPHICAL TRANSACTIONS OF THE ROYAL SOCIETY A MATHEMATICAL, PHYSICAL & ENGINEERING SCIENCES

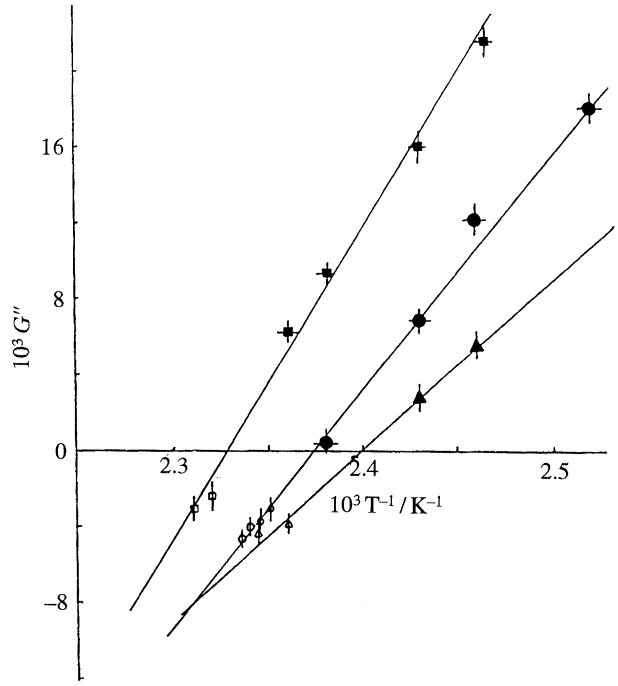

Figure 8. G'' against T^{-1} combining data from the one-phase region (closed symbols) with kinetic data (open symbols). Reprinted with permission from Higgins *et al.* (1989). Copyright American Chemical Society.

values of d_m were too small for observation by light scattering but fall conveniently in the neutron scattering range. Figure 8 offers an explanation for this, since the temperature dependence of G'' is rather steep. Thus, inside the spinodal, G'' quickly becomes large, giving large values of Q_m and small phase sizes. Generally, then, if a sample is heated through the spinodal, it is the temperature gradient of G'' which will determine the size scale of the subsequent phase separation and this, in turn, depends on the nature of the interactions between the polymers. If the sample is heated continuously during a processing operation, however, or heated and cooled, or if a chemical curing process is occurring simultaneously (as in the epoxy blends) then the rate at which the phase separation occurs will also be important, and hence M, the combined mobility term.

In recent years it has become evident that another factor in the processing conditions can affect the phase separation – its rheological history. If a partly miscible blend is placed between two microscope slides on a hot stage then, as the spinodal temperature is reached, the phase separation can be directly observed as the sample goes cloudy. If the top slide is gently pushed with a finger the sample goes clear as it is sheared and then cloudy again as the shearing stops. This surprising interaction of rheology and thermodynamics has been explored both experimentally and theoretically in recent years by us and others working in the area (see, for example, Katsaros *et al.* 1989; Lyngae-Jorgenssen & Sondergaard 1987; Hindawi *et al.* 1992; Fernández *et al.* 1993; Nakatani *et al.* 1990; Horst & Wolf 1991, 1992, 1993).

From our work it has become clear that the phase boundary can be either

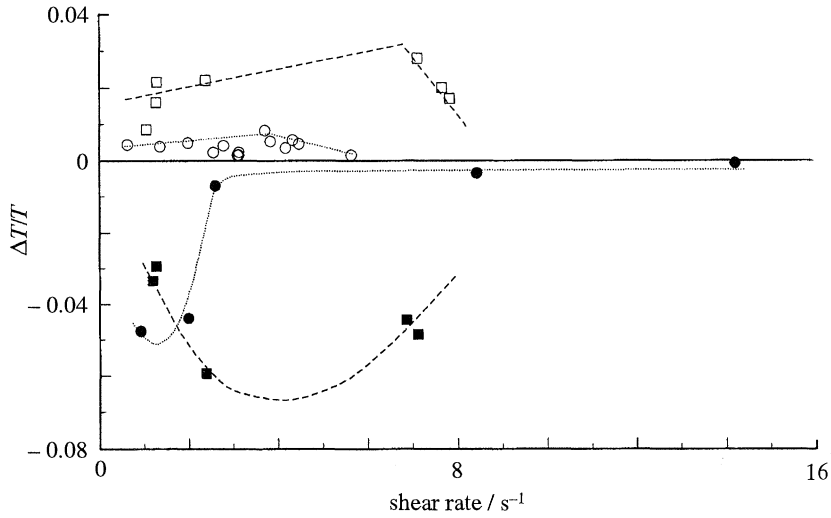

Figure 9. Normalized shift in cloud point curve as a function of shear rate for the system polystyrene polyvinyl methylether at high M_w (squares) and low M_w (circles). Reprinted with permission from Fernandez *et al.* (1993).

lowered or raised by different shear rates or more generally that islands of immiscibility can appear separated from the main spinodal curve. These are manifested by a sample becoming cloudy, then clearing, then becoming cloudy again as it is heated continuously under shear. Figure 9 shows the lower and upper cloud points which appear when a mixture of polystyrene with polyvinylmethyl ether is heated at low shear rates (Fernández *et al.* 1993) . One possible explanation of these results, that the domains are merely broken up to sizes too small to be observed by light scattering, was eliminated by examining the T_g values of quenched samples. Those from the supposed one-phase region under shear indeed showed one glass transition while those from the new two-phase region showed two transitions corresponding to the two coexisting phases (Hindawi *et al.* 1992).

Horst & Wolf (1991, 1992, 1993) have provided an explanation of these effects by adding to the free energy of mixing an extra energy term, corresponding to the elastic stored energy in the system. Depending on the concentration dependence of this term it can either remove the region of negative curvature of ΔG_m in the inset of figure 1, thus making a system exist in a single phase, or add such a region to a ΔG_m which previously showed only one minimum, causing it to become two phase. Examples of the predicted phase diagrams are shown in figure 10. Horst & Wolf have had considerable success in fitting data such as that shown in figure 9 (Fernández *et al.* 1994 *a*).

In recent experiments (Fernández *et al.* 1994 *b*) we have been investigating the whole 2D scattering pattern of the phase separating sample (rather than a 1D cut through this as, for example, in figure 6). We have also observed the sample directly through a microscope with a video attachment. Under shear and a temperature range from *ca.* 8 °C below to about 2 or 3 °C above the spinodal an unusual 'dynamic ripple pattern' was observed for PS–PVME blends, which gives rise to an intense streak in the scattering pattern. These ripples and the streak were superimposed on the normal phase separated morphology and scat-

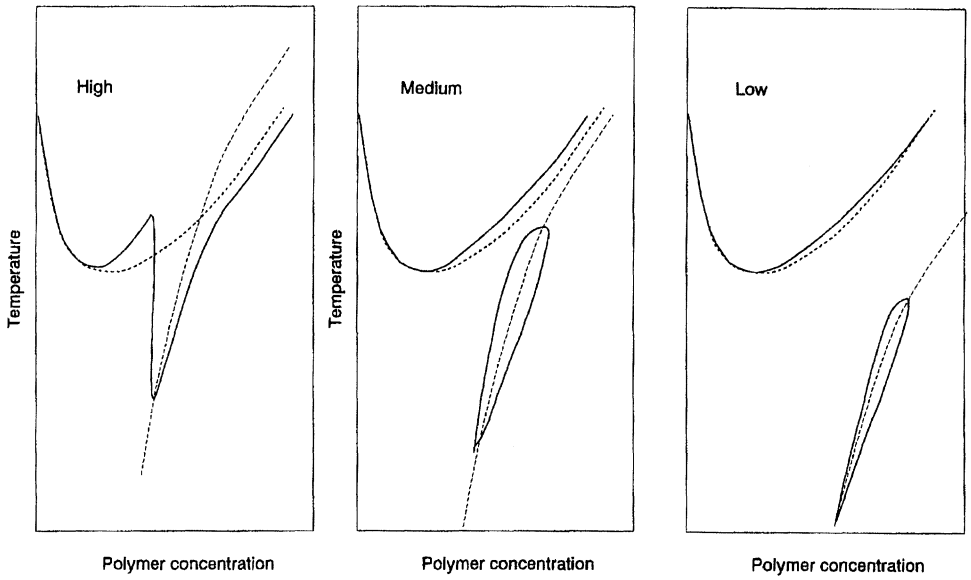

Figure 10. Theoretical prediction of the effect of shear flow on the miscibility behaviour of polymer solutions by Horst *et al.* (1993).

tering pattern for samples at $T > T_c$, and for $T < T_c$ the sample remained transparent. The ripples were typically 100 μm long by 5 μm wide. Examples of the micrographs and the scattering patterns are shown in figure 11.

We do not have a final explanation for the pattern, but the very large size of the ripples, and their rapid appearance in the sample (*ca.* 5 s after applying shear) lead us to conclude that they are not phase separation phenomena. We suggest they are more likely to be caused by flow instabilities in the sample, and may be surface phenomena. Similar scattering patterns have been reported for polymer solutions, which may or may not be due to the same phenomena (Hashimoto *et al.*, 1990). In these later cases the much higher mobility of the samples means an explanation based on gross phase separation is not as unlikely as in our case.

5. Summary

Many high molecular mass polymer mixtures are only thermodynamically miscible over a limited range of temperature and composition. Most of these are single phase at low temperatures and two phase at high temperatures. Given that polymers are glassy or partly crystalline around room temperature, and, in many cases up to much higher temperatures this often can mean that the phase diagram is not observable in practice. Clearly, if the T_g or T_m values for a mixture cross any part of the phase diagram in figure 1, that part which falls below the transitions is unobservable. Even if the transitions fall below the binodal, it can be very difficult to obtain the thermodynamic mixed state by mechanical means since polymers usually have to be well above T_g to be processed in mixers and extruders. When we add to this the complication that the shear flows encountered during the mixing process may themselves alter the phase diagram it becomes

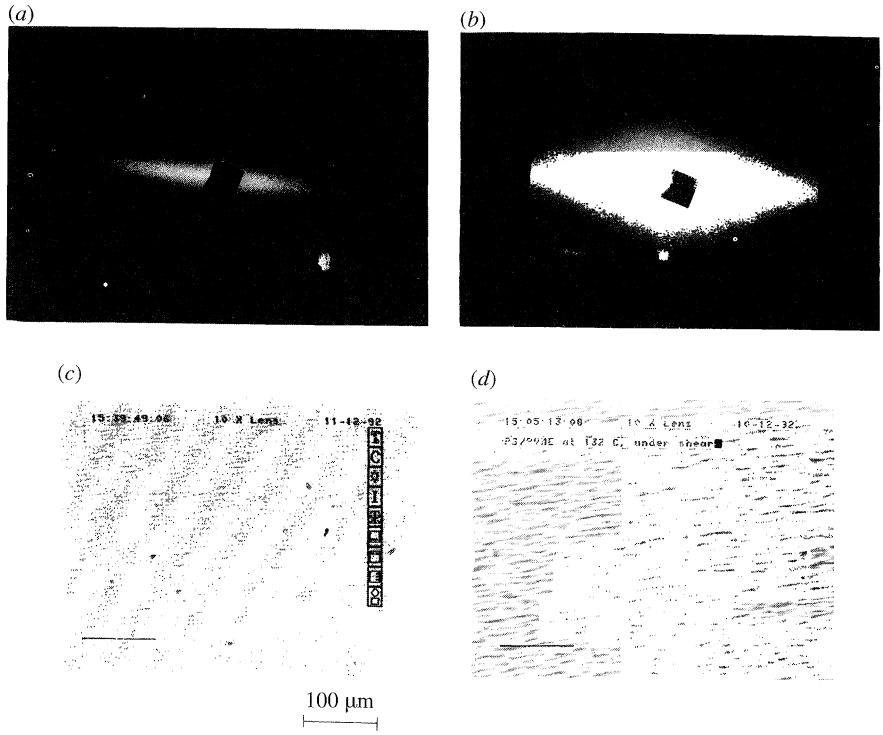

Figure 11. (*a*) Two-dimensional scattering pattern for a sample similar to that in (*c*). The sample was sheared at $\dot{\gamma} \sim 6\ \mathrm{s}^{-1}$ and $T = 126\,^{\circ}\mathrm{C}$ for 40 s. The small angle scattering signal has disappeared, but the streak arising from the wave-like structure remains. Similar results were obtained for other samples sheared in the range indicated in (*c*). (*b*) Two-dimensional scattering pattern for a sample similar to that in (*d*). The sample was sheared at $\dot{\gamma} \sim 3\ \mathrm{s}^{-1}$ and $T = 132\,^{\circ}\mathrm{C}$ for 10 s. The pattern shows a very intense streak perpendicular to the flow direction. Superimposed on this is a small angle scattering signal. Similar results were obtained for other samples sheared in the range indicated in (*d*). (*c*) Optical micrograph obtained for a sample of PS–PVME sheared at $T = 126\,^{\circ}\mathrm{C}$ and $\dot{\gamma} \sim 3\ \mathrm{s}^{-1}$ for *ca.* 10 min. The effect of shear in these conditions is to induce mixing. Correspondingly, the phase separation disappears with time but the wave-like structure remains. Similar micrographs were obtained for samples sheared in the one-phase region in the range $1\ \mathrm{s}^{-1} \leqslant \dot{\gamma} \leqslant 16\ \mathrm{s}^{-1}$ and $126\,^{\circ}\mathrm{C} \leqslant T \leqslant 129\,^{\circ}\mathrm{C}$.(*d*) Optical micrograph obtained for a sample of PS–PVME sheared at $T = 132\,^{\circ}\mathrm{C}$ and $\dot{\gamma} \sim 3\ \mathrm{s}^{-1}$ for *ca.* 10 s. The figure shows phase separation on a sub-micron scale superimposed on a wave-like structure. Similar micrographs were obtained for samples sheared in the one-phase region in the range $1\ \mathrm{s}^{-1} \leqslant \dot{\gamma} \leqslant 16\ \mathrm{s}^{-1}$ and $132\,^{\circ}\mathrm{C} \leqslant T \leqslant 136\,^{\circ}\mathrm{C}$.

evident that understanding the details of polymer polymer miscibility is vital if the resulting morphology is to be predicted and controlled.

References

Atkin, E. L., Kleintjens, L. A., Koningsveld, R. & Fetters, L. J. 1982 *Polymer Bull.* **347**.

Binder, K. 1983 *J. chem. Phys.* **79**, 6387.

Brereton, M. G., Fischer, E., Herkt-Maetzky, X. & Mortensen, K. 1987 *J. chem. Phys.* **10**, 6144.

Bucknall, C. B. & Partridge, I. 1986 *Polymer* **24**, 639.

Cahn, J. W. 1986 *Trans. metall. Soc. AIME* **242**, 169.

Carmesin, H. D., Heerman, D. W. & Binder, K. 1986 *Z. Phys.* B **65**, 89.
Clark, J. N., Fernández, M. L., Tomlins, P. E. & Higgins, J. S. 1993 *Macromolecules* **26**, 5897.
Debye, P. & Bueche, A. 1941 *J. chem. Phys.* **9**, 660.
Eichinger, B. & Flory, P. J. 1968 *Trans. Faraday Soc.* **14**, 2035.
Einstein, A. 1910 *Annln Phys. (Leipzig)* **33**, 1275.
Flory, P. J. 1941 *J. chem. Phys.* **9**, 660.
Flory, P. J., Orwell, R. A. & Vrij, A. 1964 *J. Am. chem. Soc.* **88**, 3507.
Fernández, M. L., Higgins, J. S. & Tomlins, P. E. 1989 *Polymer* **30**, 3.
Fernández, M. L., Higgins, J. S. & Richardson, S. M. 1993 *Trans. Instn chem. Engrs* A **71**, 239.
Fernández, M. L., Higgins, J. S., Horst, R. & Wolf, B. A. 1994 *a* (In the press.)
Fernández, M. L., Higgins, J. S. & Richardson, S. M. 1994 *b* (In the press.)
Graessley, W. W., Krishnamoorti, R., Babara, N. P., Fetters, L. J., Lohse, D. J., Schulz, D. N. & Sissans, J. A. 1993 *Macromolecules* **26**, 1137.
Guo, W. G. & Higgins, J. S. 1990 *Polymer* **31**, 699.
Hashimoto, T. 1993 In *Materials science and technology* (ed. R. W. Cahn, P. Haasen, E. J. Kramer), vol. 12: *Structure and properties of polymers* (ed. E. L. Thomas).
Higgins, J. S., Fruitwala, H. & Tomlins, P. E. 1989 *Macromolecules* **22**, 3674.
Hindawi, I., Higgins, J. S. & Weiss, R. A. 1992 *Polymer* **33**, 2522.
Horst, R. & Wolf, B. A. 1993 *Macromolecules* **26**, 5676.
Huston, E. L., Cahn, J. W. & Hilliard, J. E. 1966 *Acta metall* **14**, 1053.
Jones, R. A. L. 1987 Ph.D. thesis, Cambridge.
Katsaros, D., Malone, M. F. & Winter, H. H. 1989 *Polymer Engng Sci.* **29**, 1434.
Kinloch, A. J., Yuen, M. L. & Jenkins, S. D. 1993 *J. Mater. Sci.* (In the press.)
Kramer, E. J. & Composto, R. J. 1987 *Polymer Preprints (Am. Chem. Soc. Div. Pol. Chem.)* **28**, 323.
Kroschwitz, X. 1990 *Concise encyclopedia of polymer science and engineering.*
Lapp, A., Picot, C. & Benoît, H. 1985 *Macromolecules* **18**, 2437.
Lyngae-Jorgensen, J. & Sondegaard, K. 1987 *Polymer Engng Sci.* **27**, 351.
Maconnachie, A., Fried, J. R. & Tomlins, P. E. 1989 *Macromolecules* **22**, 4606.
Nakatani, A. I., Kim, H., Takahashi, Y., Matsushita, Y., Takano, A., Bauer, B. J. & Han, C. C. 1990 *J. chem. Phys.* **93**, 795.
Okada, M. & Han, C. C. 1986 *J. chem. Phys.* **85**, 5317.
Pincus, P. 1981 *J. chem. Phys.* **75**, 1996.
Shibayama, M., Yang, H., Stein, R. S. & Han, C. C. 1985 *Macromolecules* **18**, 2197.
Snyder, H. L. & Meakin, P. 1985 *J. Polymer Sci. Symp.* **73**, 217.
Strobl, G. R. 1985 *Macromolecules* **15**, 558.
Tomlins, P. E. & Higgins, J. S. 1988 *Macromolecules* **21**, 425.
Warner, M., Higgins, J. S. & Carter, A. J. 1983 *Macromolecules* **16**, 1931.
Yamanaka, K. & Inoue, T. 1989 *Polymer* **30**, 662.

Discussion

A. Keller (*University of Bristol, U.K.*). Although I cannot suggest a direct explanation for the striations seen at or around phase separation conditions. I wish to draw attention to a class of effects we observed in Bristol in the course of work on shear-induced liquid–liquid phase separation in solutions of very high molecular static polyolefins. Here, using a Couette system conspicuous happenings were registered relating to the presence of surfaces. Specifically, an

PHILOSOPHICAL TRANSACTIONS OF THE ROYAL SOCIETY A MATHEMATICAL, PHYSICAL & ENGINEERING SCIENCES

adsorbtion layer which kept on thickening during shear (termed by us 'adsorbtion entanglement layer'). It was directly registerable when looking down parallel to the cylinder walls and was causing pronounced changes in the viscosity while building up during shear. This adsorbtion entanglement layer could then initiate liquid–liquid phase separation under appropriate conditions (temperature, concentration) when the same would not have taken place in the stationary state. Clearly, here the adsorbtion layer nucleates the phase separtaion pointing, among others, to the significant role that surfaces can play (P.J. Barnham & A. Keller, *Macromolecules* **23**, 303 (1990)). In addition to being of interest in their own rights, such effects serve to draw attention to possibilities along surfaces when encountering phenomena that are inexplicable otherwise.

J. S. Higgins. I am inclined to suspect surface effects are important either as a cause of the ripple pattern, or facilitating their dynamics. It is well know that in polymer mixtures a surface layer of one or other component may occur if there are large differences in surface activity. Moreover, R. Jones *et al.* (*Phys. Rev. Lett.* **66**, 1326 (1991)) have reported surface activated phase separation in polymer blends where the usual spinodal pattern is replaced in a thin film by oscillations in concentration perpendicular to the surface. A thin layer rich in the lower viscosity component could become unstable when the sample is sheared and show the wave like effects observed.

C. B. Bucknall (*Cranfield University, U.K.*). Have you considered birefringence as a possible cause of the ripple patterns that you observe during shear of polystyrene/PVME blends? If the system is developing minor inhomogeneities on the scale of 10 to 100 μm in the region of the LCST, spatial and temporal variations in optical properties could arise as a result of extension and relaxation over a period of seconds. This explanation would avoid the need to postulate mass transfer over impossibly large distances in the same timescale. A test of the hypothesis would be to examine polymers with a range of strain-optical behaviour. A solution of PMMA in liquid epoxy resin (diglycidyl ether of Bisphenol A) should be relatively ineffective in producing ripples because of the low birefringence of PMMA.

J. S. Higgins. We have considered birefringence as a possible cause, although we are not as yet using polarized light. We will be investigating this in more detail in the future. A blend of ethylene-vinyl acetate copolymer with solution chlorinated polyethylene did not show a ripple pattern under similar flow conditions but this may be because the rheology is very different from that of the PS–PVME system reported in the paper.

A. H. Windle (*Cavendish Laboratory, U.K.*). In the case of the small molecule solutions or atomic alloys, a single phase field is invariably stabilized by entropy. On the other hand, a single phase polymer blend, at a temperature which is below the lower critical temperature, is rather special. It must be stabilized by some sort of enthalpic interaction between dissimilar molecules which will be vulnerable to increasing temperature. One view of such positive interactions is that there are particular bonds which are formed between localized regions of each dissimilar molecule. If such special positioning is required, then it is likely to be disrupted by shear as well as by temperature, rather as a material such as non-drip paint

PHILOSOPHICAL TRANSACTIONS OF THE ROYAL SOCIETY A MATHEMATICAL, PHYSICAL & ENGINEERING SCIENCES

loses its thixotropic 'set' if it is stirred. In this perspective, it would perhaps be more surprising if segregation into two phases under shear did not occur.

J. S. Higgins. I had always taken a 'molecular' view of blend miscibility, and in many high M_w partly miscible systems, specific interactions are involved. Although the explanation of shear effects based on a 'macroscopic' view of elastic-stored energy contributions does fit the experimental facts, I would like to see a detailed analysis based on the effect of these specific interactions.

PHILOSOPHICAL TRANSACTIONS OF THE ROYAL SOCIETY A MATHEMATICAL, PHYSICAL & ENGINEERING SCIENCES

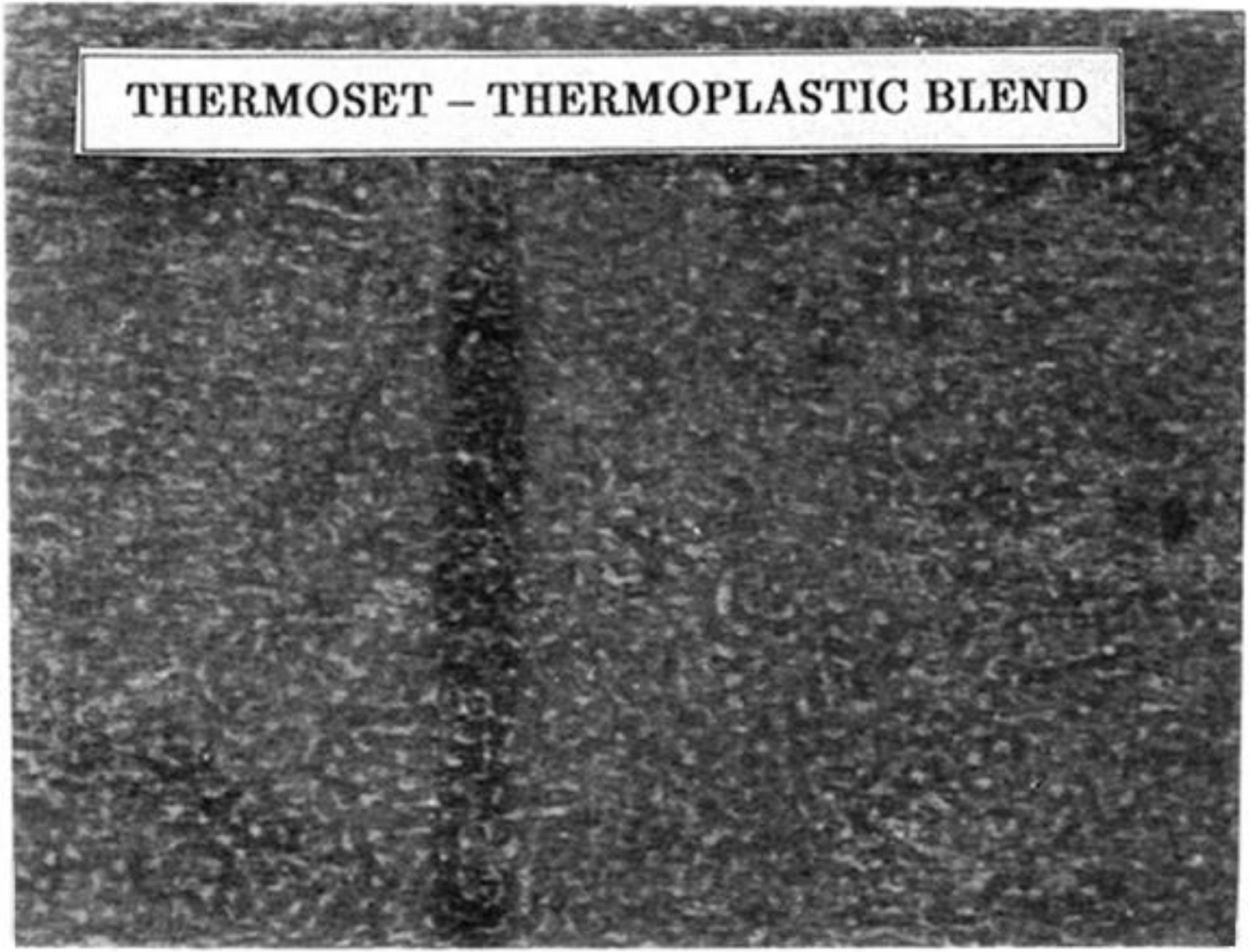

gure 5. Optical micrograph of a Thermoset–thermoplastic blend provided by ICI plc. Magnification ×20.

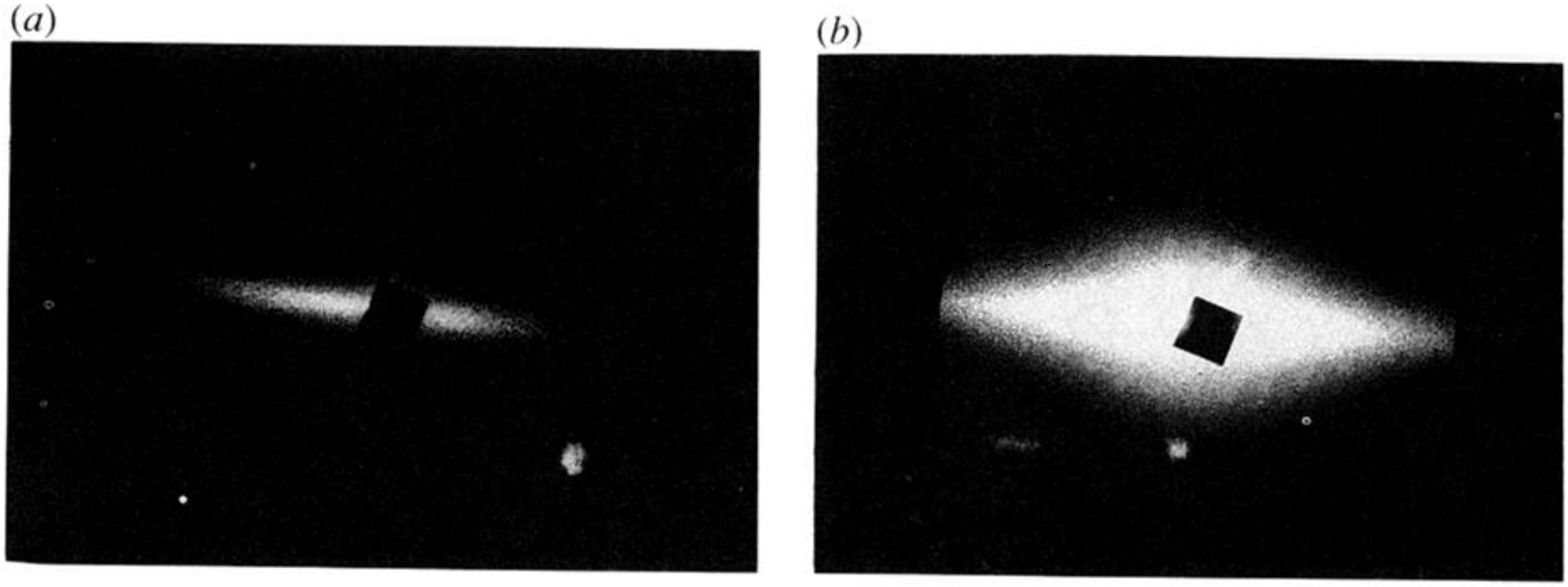

Figure 11. (*a*) Two-dimensional scattering pattern for a sample similar to that in (*c*). The sample was sheared at $\dot{\gamma} \sim 6\ \mathrm{s}^{-1}$ and $T = 126\,^{\circ}\mathrm{C}$ for 40 s. The small angle scattering signal has disappeared, but the streak arising from the wave-like structure remains. Similar results were obtained for other samples sheared in the range indicated in (*c*). (*b*) Two-dimensional scattering pattern for a sample similar to that in (*d*). The sample was sheared at $\dot{\gamma} \sim 3\ \mathrm{s}^{-1}$ and $T = 132\,^{\circ}\mathrm{C}$ for 10 s. The pattern shows a very intense streak perpendicular to the flow direction. Superimposed on this is a small angle scattering signal. Similar results were obtained for other samples sheared in the range indicated in (*d*). (*c*) Optical micrograph obtained for a sample of PS–PVME sheared at $T = 126\,^{\circ}\mathrm{C}$ and $\dot{\gamma} \sim 3\ \mathrm{s}^{-1}$ for *ca.* 10 min. The effect of shear in these conditions is to induce mixing. Correspondingly, the phase separation disappears with time but the wave-like structure remains. Similar micrographs were obtained for samples sheared in the one-phase region in the range $1\ \mathrm{s}^{-1} \leqslant \dot{\gamma} \leqslant 16\ \mathrm{s}^{-1}$ and $126\,^{\circ}\mathrm{C} \leqslant T \leqslant 129\,^{\circ}\mathrm{C}$.(*d*) Optical micrograph obtained for a sample of PS–PVME sheared at $T = 132\,^{\circ}\mathrm{C}$ and $\dot{\gamma} \sim 3\ \mathrm{s}^{-1}$ for *ca.* 10 s. The figure shows phase separation on a sub-micron scale superimposed on a wave-like structure. Similar micrographs were obtained for samples sheared in the one-phase region in the range $1\ \mathrm{s}^{-1} \leqslant \dot{\gamma} \leqslant 16\ \mathrm{s}^{-1}$ and $132\,^{\circ}\mathrm{C} \leqslant T \leqslant 136\,^{\circ}\mathrm{C}$.